

**MODIFICATION OF MULTI-WALLED CARBON NANOTUBES FOR  
PERVAPORATION NANOCOMPOSITE MEMBRANE**

**by**

**ONG YIT THAI**

**Thesis submitted in fulfillment of the  
requirements for the degree of  
Master of Science**

**February 2011**

## ACKNOWLEDGEMENT

First of all, I would like to express my deepest and most heart-felt gratitude to my beloved parents and siblings for their endless love and encouragement throughout my entire master degree program.

Secondly, I would like to give my sincere thanks to my dedicated supervisors Dr. Tan Soon Huat and Prof. Dr. Abdul Latif Ahmad for their excellent supervision and enormous effort spent in guiding and helping me throughout my studies. My accomplishment of this research project is a direct reflection of high quality supervision work from both of my supervisors.

Thirdly, I would like to express my gratitude to the administrative staff of School of Chemical Engineering, Universiti Sains Malaysia especially our respected dean, Prof. Dr. Azlina Harun @ Kamaruddin, deputy dean, office staffs and technicians for giving me full support throughout my research work.

Fourthly, I would to show my deepest gratitude and thanks to all my beloved friends and colleagues: Man Kee, Kian Fei, Wei Ming, Kam Chung, Siew Hoong, Henry, Mun Sing, Sie Yon, Kim Yang, Kah Ling, Chiew Hwee, Lee Chung, and Thiam Leng for their unparalleled help, kindness and moral support towards me. Not forgotten are my juniors: Chin Wei, Kok Hong, Yoke Kooi and others for their sincere support given to me. I might not able to achieve what I want to be without the support from all of my colleagues.

Last but not least, the financial support from Universiti Sains Malaysia Research University Grant via the Golden Goose project, Ministry of Science, Technology and Innovation (MOSTI), Fundamental Research Grant Scheme (FRGS), USM Fellowship and USM Research University Postgraduate Research Grant Scheme (USM-RU PRGS) is gratefully acknowledged.

Thank you very much!

***Ong Yit Thai, 2011***

## TABLE OF CONTENTS

|  | Page |
|--|------|
| <b>ACKNOWLEDGEMENT</b>   | ii   |
| <b>LIST OF TABLES</b>  | vii  |
| <b>LIST OF FIGURES</b>   | ix   |
| <b>LIST OF ABBREVIATIONS</b>                                       | xii  |
| <b>LIST OF SYMBOLS</b>   | xiii |
| <b>ABSTRAK</b>   | xiv  |
| <b>ABSTRACT</b>  | xvi  |
| <br>   |      |
| <b>CHAPTER 1 - INTRODUCTION</b>                                    |      |
| 1.1 Pervaporation  | 1    |
| 1.2 Biodegradable Polymer  | 5    |
| 1.3 Chitosan   | 8    |
| 1.4 Problem Statement  | 11   |
| 1.5 Objectives   | 12   |
| 1.6 Scope of Study   | 13   |
| 1.7 Organization of the Thesis                                     | 14   |
| <br>   |      |
| <b>CHAPTER 2 - LITERATURE REVIEW</b>                               |      |
| 2.1 Brief Introduction on Carbon Nanotubes                         | 16   |
| 2.2 Properties of Carbon Nanotubes                                 | 18   |
| 2.3 Carbon Nanotubes as Reinforcing Agent in Polymer Nanocomposite | 20   |
| 2.4 Fabrication of Carbon Nanotube/Polymer Nanocomposite           | 24   |
| 2.5 Modification of Carbon Nanotubes for Polymer Nanocomposite     | 26   |
| 2.5.1 Functionalization of Carbon Nanotubes                        | 27   |
| 2.5.2 Alignment of Carbon Nanotubes                                | 31   |
| 2.6 Application of Chitosan in Pervaporation Process               | 34   |
| 2.7 Poly-3-hydroxybutyrate   | 38   |
| 2.8 Fundamental of Pervaporation Process                           | 41   |
| 2.9 Dehydration of 1,4-dioxane                                     | 43   |

|        |                                   |    |
|--------|-----------------------------------|----|
| 2.10   | Statistical Design of Experiments | 46 |
| 2.10.1 | Response Surface Methodology      | 46 |
| 2.10.2 | Central Composite Design          | 47 |

### **CHAPTER 3 - MATERIALS AND METHODOLOGY**

|       |   |    |
|-------|---|----|
| 3.1   | Raw Materials and Chemicals   | 51 |
| 3.1.1 | Raw Materials   | 51 |
| 3.1.2 | Chemicals   | 51 |
| 3.2   | Process Study   | 53 |
| 3.3   | Functionalization of MWCNTs   | 53 |
| 3.4   | Synthesis of Homogeneous and Aligned PHB-MWCNT in Chitosan Membrane | 54 |
| 3.5   | Pervaporation Performances  | 56 |
| 3.6   | Design of Experiment (DOE)  | 61 |
| 3.7   | Characterization  | 63 |
| 3.7.1 | Thermogravimetric Analysis (TGA)                                    | 63 |
| 3.7.2 | Fourier Transform Infrared Spectroscopy (FTIR)                      | 63 |
| 3.7.3 | Scanning Electron Microscopy (SEM)                                  | 64 |
| 3.7.4 | Transmission Electron Microscopy (TEM)                              | 64 |
| 3.7.5 | Dispersion Study  | 64 |
| 3.7.6 | Mechanical Properties of the Membranes                              | 64 |
| 3.7.7 | Liquid Sorption Studies   | 65 |

### **CHAPTER 4 - RESULTS AND DISCUSSION**

|       |   |    |
|-------|---|----|
| 4.1   | Characterization                        | 66 |
| 4.1.1 | Thermogravimetric Analysis              | 66 |
| 4.1.2 | Fourier Transform Infrared Spectroscopy | 69 |
| 4.1.3 | Transmission Electron Microscopy        | 71 |
| 4.1.4 | Dispersion Study                        | 72 |
| 4.1.5 | Scanning Electron Microscopy            | 73 |
| 4.1.6 | Mechanical Properties of the Membranes  | 78 |
| 4.1.7 | Liquid Sorption Studies                 | 80 |

|  |   |     |
|--|---|-----|
| 4.2  | Pervaporation Performances  | 82  |
| 4.2.1  | Effect of Feed Concentration  | 82  |
| 4.2.2  | Effect of Feed Temperature  | 85  |
| 4.2.3  | Effect of Downstream Pressure   | 89  |
| 4.3  | Design of Experiment  | 92  |
| 4.3.1  | Statistical Analysis of Results   | 92  |
| 4.3.2  | Development of Regression Model Equation  | 96  |
| 4.3.3  | Effect of Individual Operating Parameter on Pervaporation Process for 1,4-dioxane Dehydration using PHB-MWCNT/Chitosan Nanocomposite Membrane               | 99  |
| 4.3.4  | Effect of Interaction Between the Operating Parameters on Pervaporation Process for 1,4-dioxane Dehydration using PHB-MWCNT/Chitosan Nanocomposite Membrane | 105 |
| 4.4  | Process Optimization Studies  | 113 |
| <br><b>CHAPTER 5 - CONCLUSIONS AND RECOMMENDATIONS</b> |   |     |
| 5.1  | Conclusions   | 121 |
| 5.2  | Recommendations   | 122 |
| <br><b>References</b>                                  |   | 124 |
| <br><b>Appendices</b>                                  |   | 138 |
| <br><b>List of Publications</b>                        |   | 139 |

## LIST OF TABLES

|           |  | Page |
|-----------|--|------|
| Table 1.1 | Summary of the membrane separation technologies.   | 1    |
| Table 1.2 | Principal applications of chitosan.  | 10   |
| Table 2.1 | Overview of the important synthesis procedures for carbon Nanotubes.   | 18   |
| Table 2.2 | Performance of various polymeric membranes in dehydration of 1,4-dioxane.  | 45   |
| Table 3.1 | Lists of chemicals.  | 52   |
| Table 3.2 | Experiment data on the influence of operating parameters.  | 60   |
| Table 3.3 | Experimental range and level for the operating parameters.   | 61   |
| Table 3.4 | Experimental data on study influence of operating parameter and process optimization using DOE.  | 62   |
| Table 4.1 | Mechanical properties of chitosan, raw MWCNT/chitosan and PHB-MWCNT/chitosan nanocomposite membrane.   | 79   |
| Table 4.2 | Pervaporation result of chitosan and PHB-MWCNT/chitosan nanocomposite membrane in dehydration of 1,4-dioxane at various feed concentration.  | 82   |
| Table 4.3 | Pervaporation result of chitosan and PHB-MWCNT/chitosan nanocomposite membrane in dehydration of 1,4-dioxane at various feed temperature.    | 85   |
| Table 4.4 | Permeation activation energies for chitosan and PHB-MWCNT/chitosan nanocomposite membrane at different temperatures.                         | 88   |
| Table 4.5 | Pervaporation result of chitosan and PHB-MWCNT/chitosan nanocomposite membrane in dehydration of 1,4-dioxane at various downstream pressure. | 90   |
| Table 4.6 | Experiment runs and response for the pervaporation dehydration of 1,4-dioxane using PHB-MWCNT/chitosan nanocomposite membrane.               | 93   |

|            |   |     |
|------------|---|-----|
| Table 4.7  | ANOVA results for regression model equation and coefficients of model terms for permeation flux of PHB-MWCNT/chitosan nanocomposite membrane.                                 | 95  |
| Table 4.8  | ANOVA results for regression model equation and coefficients of model terms for selectivity of PHB-MWCNT/chitosan nanocomposite membrane.                                     | 95  |
| Table 4.9  | Optimization criteria for permeation flux in the pervaporation process of 1,4-dioxane dehydration using PHB-MWCNT/chitosan nanocomposite membrane.                            | 115 |
| Table 4.10 | Optimization criteria for selectivity in the pervaporation process of 1,4-dioxane dehydration using PHB-MWCNT/chitosan nanocomposite membrane.                                | 115 |
| Table 4.11 | Optimization criteria for combination of permeation flux and selectivity in pervaporation process of 1,4-dioxane dehydration using PHB-MWCNT/chitosan nanocomposite membrane. | 115 |
| Table 4.12 | Verification experiments on optimum condition for the pervaporation process of 1,4-dioxane dehydration using PHB-MWCNT/chitosan nanocomposite membrane.                       | 117 |
| Table 4.13 | Comparison of the dehydration performance of chitosan, PHB-MWCNT/chitosan and non- bulk aligned PHB-MWCNT/chitosan under the optimum condition.                               | 119 |
| Table A.1  | Mechanical properties of non-aligned PHB-MWCNT/chitosan nanocomposite membrane.   | 138 |



## LIST OF FIGURES

|            |   | Page |
|------------|---|------|
| Figure 1.1 | Overview of the pervaporation for aqueous organic mixtures.   | 2    |
| Figure 1.2 | Flowchart on different type of Pervaporation processes.   | 4    |
| Figure 1.3 | Life cycles of biodegradable polymers.  | 6    |
| Figure 1.4 | Chemical structure of chitosan  | 8    |
| Figure 2.1 | (a) Schematic diagram showing the possible wrapping of the 2D graphene sheet into tubular forms, (b) an armchair-type nanotube, (c) a zigzag-type nanotube, and (d) a chiral-type nanotube.   | 17   |
| Figure 2.2 | Number of published journal articles relate to CNTs/Polymer nanocomposite as a function of year.  | 21   |
| Figure 2.3 | Functionalization possibilities for CNTs: A) defect-group functionalization, B) covalent sidewall functionalization, C) noncovalent exohedral functionalization with surfactant, D) noncovalent exohedral functionalization with polymers, and E) endohedral functionalization. | 28   |
| Figure 2.4 | a) MWCNT-PS, and b) MWCNT-PMMA. MWCNTs were wrapped by polymer chain as indicated by arrows.  | 30   |
| Figure 2.5 | Chemical structure of Poly-3-hydroxybutyrate (PHB).   | 38   |
| Figure 3.1 | Schematic diagram for overall research methodology.   | 50   |
| Figure 3.2 | Schematic diagram on the fabrication of the PHB-MWCNT/chitosan nanocomposite membrane.  | 56   |
| Figure 3.3 | Schematic representation of pervaporation apparatus.  | 57   |
| Figure 4.1 | Thermogravimetric thermogram on (a) raw MWCNT, (b) oxidized MWCNT, (c) PHB-MWCNT.   | 67   |
| Figure 4.2 | Thermogravimetric thermogram of PHB-MWCNT after each washing cycle.   | 69   |
| Figure 4.3 | FTIR spectra for raw MWCNT, oxidized MWCNT, PHB-MWCNT and PHB.  | 70   |

|             |  |     |
|-------------|--|-----|
| Figure 4.4  | TEM images (a) oxidized MWCNT, and (b) PHB-MWCNT.  | 72  |
| Figure 4.5  | Dispersion test of raw MWCNT, oxidized MWCNT and PHB-MWCNT in (a) ethanol and (b) chloroform.  | 73  |
| Figure 4.6  | Schematic diagram on bulk aligned PHB-MWCNT in chitosan matrix.  | 73  |
| Figure 4.7  | SEM image on (a) surface view of chitosan, (b) cross sectional view of chitosan, (c) surface view of raw MWCNT/chitosan, (d) cross sectional view of raw MWCNT/chitosan, (e) surface view of PHB-MWCNT/chitosan, (d) cross sectional view of PHB-MWCNT/chitosan. | 75  |
| Figure 4.8  | Degree of swelling for chitosan and PHB-MWCNT/chitosan nanocomposite membranes.  | 81  |
| Figure 4.9  | (a) Permeation flux and (b) selectivity of chitosan and PHB-MWCNT/chitosan membrane, as a function of feed concentration of water.   | 83  |
| Figure 4.10 | (a) Permeation flux and (b) selectivity of chitosan and PHB-MWCNT/chitosan membrane, as a function feed temperature.   | 86  |
| Figure 4.11 | The Arrhenius plot of semi-logarithmic plot of permeation flux against the reciprocal of the absolute temperature.   | 88  |
| Figure 4.12 | (a) Permeation flux and (b) selectivity of chitosan and PHB-MWCNT/chitosan membrane, as a function of downstream pressure.   | 91  |
| Figure 4.13 | Parity plot between actual permeation flux and predicted permeation flux.  | 98  |
| Figure 4.14 | Parity plot between actual selectivity and predicted selectivity.  | 98  |
| Figure 4.15 | Individual effect of feed concentration of water on (a) permeation flux and (b) selectivity of PHB-MWCNT/chitosan nanocomposite membrane at 30°C and 5 mmHg.   | 101 |
| Figure 4.16 | Individual effect of feed temperature on (a) permeation flux and (b) selectivity of PHB-MWCNT/chitosan nanocomposite membrane at 15 mmHg and 10.5 wt.% feed concentration of water.  | 103 |

|             |   |     |
|-------------|---|-----|
| Figure 4.17 | Individual effect of downstream pressure on (a) permeation flux and (b) selectivity of PHB-MWCNT/chitosan nanocomposite membrane at 30°C and 10.5 wt.% feed concentration of water.                         | 104 |
| Figure 4.18 | Interaction effect between feed temperature and feed concentration of water on permeation flux of PHB-MWCNT/chitosan nanocomposite membrane shown as (a) interaction plot and (b) response surface plot.    | 106 |
| Figure 4.19 | Interaction effect between downstream pressure and feed concentration of water on permeation flux of PHB-MWCNT/chitosan nanocomposite membrane shown as (a) interaction plot and (b) response surface plot. | 108 |
| Figure 4.20 | Interaction effect between feed temperature and downstream pressure on selectivity of PHB-MWCNT/chitosan nanocomposite membrane shown as (a) interaction plot and (b) response surface plot.                | 110 |
| Figure 4.21 | Interaction effect between downstream pressure and feed concentration of water on selectivity of PHB-MWCNT/chitosan nanocomposite membrane shown as (a) interaction plot and (b) response surface plot.     | 112 |
| Figure A.1  | Non-bulk aligned PHB-MWCNT/chitosan nanocomposite membrane.   | 138 |

## LIST OF ABBREVIATIONS

|         |   |
|---------|---|
| AFM     | Atomic force microscopy                       |
| ANOVA   | Analysis of variance                          |
| ASTM    | American Society for Testing and Materials    |
| CCD     | Central composite design                      |
| CI      | Confidence interval                           |
| CNTs    | Carbon nanotubes                              |
| COCl    | Acyl chloride                                 |
| CVD     | Chemical vapor decomposition                  |
| DOE     | Design of experiment                          |
| DSC     | Differential scanning calorimetry             |
| FT-IR   | Fourier transform infrared spectroscopy       |
| F-value | Fisher test value                             |
| GA      | Glutaraldehyde                                |
| GPTMS   | $\gamma$ -(glycidyloxypropyl)trimethoxysilane |
| HEC     | Hydroxyethylcellulose                         |
| HFIP    | 1,1,1,3,3,3-hexafluoro-2-propanol             |
| ISO     | International Standards Organization          |
| LCA     | Life-cycle assessment                         |
| LMCS    | Low molecular weight chitosan                 |
| MWCNTs  | Multiwalled carbon nanotubes                  |
| NaAlg   | Sodium alginate                               |
| NMR     | Nuclear magnetic resonance spectroscopy       |
| PAA     | Poly(acrylic acid)                            |
| PDMS    | Polydimethylsiloxane                          |
| PEI     | Polyetherimide                                |
| PHA     | Polyhydroxyalkanoate                          |
| PHB     | Poly-3-hydroxybutyrate                        |
| PLLA    | Poly(L-lactide)                               |
| PMMA    | Poly(methyl methacrylate)                     |
| Prob    | Probability                                   |
| PSPEO   | Siloxane polyether copolymer                  |
| PTFE    | Poly(tetrafluoroethylene)                     |
| PVA     | Poly(vinyl alcohol)                           |
| RSM     | Response surface methodology                  |
| SEM     | Scanning electron microscopy                  |
| SWCNTs  | Single-walled carbon nanotubes                |
| TDI     | Toluylene-2,4-diisocyanate                    |
| TEM     | Transmission electron microscopy              |
| TGA     | Thermogravimetric analysis                    |
| THF     | Tetrahydrofuran                               |

## LIST OF SYMBOLS

|               |  |
|---------------|--|
| $\alpha$      | Selectivity  |
| $\varepsilon$ | Error  |
| $A$           | Coded term of feed temperature   |
| $B_0$         | Constant   |
| $B$           | Coded term of downstream pressure  |
| $C$           | Coded term of feed concentration of water                                  |
| $B_i$         | Linear coefficients in Equation (2.8)                                      |
| $B_{ii}$      | Quadratic coefficients in Equation (2.8)                                   |
| $B_{ij}$      | Interaction coefficient in Equation (2.8)                                  |
| $Q$           | Quantity in gram of the permeate collected                                 |
| $\Delta t$    | Time interval of pervaporation process                                     |
| $A$           | Effective membrane area  |
| $J_0$         | Pre-exponential factor   |
| $x_i, x_j$    | Variable corresponding to factor in Equation (2.8)                         |
| $Y$           | Response calculated in Equation (2.8)                                      |
| $C_m, C$      | Concentrations of a species in the membrane surface and the feed.          |
| $K$           | Partition coefficient of a species between the membrane and the feed phase |
| $J$           | Permeation flux  |
| $D$           | Diffusion coefficient  |
| $\Delta C$    | Transmembrane concentration  |
| $E_a$         | Permeation activation energy   |
| $R$           | Gas constant   |
| $T$           | Absolute feed temperature  |

# PENGUBAHSUAIAN TIUB-NANO KARBON DINDING BERLAPIS UNTUK MEMBRAN KOMPOSIT-NANO PERVAPORASI

## ABSTRAK

Pervaporasi semakin mendapat perhatian dalam teknologi pemisahan membran kerana penggunaan tenaga yang rendah, operasi dan kawalan yang mudah. Disebabkan keperluan bagi membran pervaporasi yang berprestasi tinggi and kemunculan polimer biodegradasi, kitosan telah menjadi salah satu membran pervaporasi biodegradasi yang paling banyak dikaji. Tetapi, membran kitosan tulen biasanya mengalami kememilihan yang sangat rendah akibat pengampulan membran. Dalam kajian ini, tiub-nano karbon dinding berlapis (MWCNTs) dicadangkan untuk digabungkan ke dalam matriks kitosan sebagai satu cara untuk mengurangkan pengampulan membran kitosan. Penghasilan membran komposit-nano MWCNT/kitosan yang berkualiti tinggi adalah sukar kerana ia memerlukan penyerakan MWCNTs yang homogen dan teratur. Justeru itu, kajian ini telah menghasilkan MWCNTs yang mengandungi keberangkapan poly(3-hydroxybutyrate) (PHB), sejenis polimer biodegradasi yang boleh-larut campur dengan kitosan supaya dapat meningkatkan keserasian dan penyerakan MWCNTs dalam matriks kitosan. Keputusan dari analisis termogravimetri (TGA) dan mikroskop transmisi elektron (TEM) menunjukkan bahawa sebanyak 40 peratusan berat PHB telah berjaya dilekatkan pada MWCNTs melalui balutan permukaan. Selain itu, untuk mengoptimumkan kesan penguatan MWCNTs yang mengandungi keberangkapan PHB (PHB-MWCNT), ia telah disusunkan secara pukal melalui kaedah penapisan mudah. Penyusunan tersebut boleh mengurangkan jumlah MWCNTs yang diperlukan untuk mencapai sifat mekanik yang dikehendaki. Apabila menggunakan membran komposit-nano PHB-MWCNT/kitosan dalam dehidrasi 1,4-

dioxane, membran komposit-nano tersebut mempamerkan penambahan dalam kememilihan terhadap air dan penurunan fluks penelapan ketika menambah kepekatan 1,4-dioxane dalam larutan suapan. Namun penambahan suhu suapan menurunkan kememilihan membran komposit-nano tetapi meningkatkan fluks penelapan. Semasa dikenakan tekanan hilir yang tinggi (vakum rendah), kedua-dua kememilihan dan fluks penelapan menurun akibat kekurangan daya pergerakan. Berbanding dengan membran kitosan, pergabungan PHB-MWCNT jelas meningkatkan penelapan tetapi mengorbankan kememilihan membran. Akhirnya, keadaan optimum membran komposit-nano dalam proses dehidrasi 1,4-dioxane diperolehi dengan menggunakan metodologi permukaan sambutan (RSM). Optimum fluks penelapan dengan nilai  $69.48 \text{ g/m}^2\cdot\text{j}$  dapat diperolehi dengan  $59.7^\circ\text{C}$  suhu suapan,  $5.00 \text{ mmHg}$  tekanan hilir dan  $18.88$  peratusan berat air dalam kepekatan larutan suapan. Bagi kememilihan, nilai optimum  $2292.09$  diperolehi pada  $30^\circ\text{C}$  suhu suapan,  $5.00 \text{ mmHg}$  tekanan hilir dan  $1$  peratusan berat air dalam kepekatan larutan suapan. Keseimbangan di antara fluks penelapan dan kememilihan dijangka berlaku secara serentak ketika proses pervaporasi dijalankan pada  $30$  suhu suapan,  $5.00 \text{ mmHg}$  tekanan hilir dan  $10.92$  peratusan berat air dalam kepekatan larutan suapan. Nilai optimum  $40.57 \text{ g/m}^2\cdot\text{j}$  and  $1668.48$  diperolehi bagi fluks penelapan dan kememilihan masing-masing dalam keadaan tersebut.

# MODIFICATION OF MULTI-WALLED CARBON NANOTUBES FOR PERVAPORATION NANOCOMPOSITE MEMBRANE

## ABSTRACT

Owing to its low energy consumption, operational simplicity and ease of control, pervaporation has gained increasing interest in membrane separation technology. Due to the requirement of high performance pervaporation membrane and the emergence of biodegradable polymer, chitosan has become one of the most studied biodegradable pervaporation membrane. Unfortunately, the pure chitosan membrane often suffers from low selectivity caused by excessive swelling. In this research work, it is proposed to incorporate multi-walled carbon nanotubes (MWCNTs) into chitosan matrix as an outcome to reduce the excessive swelling behaviour of chitosan. Producing a high quality MWCNT/chitosan nanocomposite membrane becomes a daunting task as it requires a homogenous dispersion of MWCNTs in uniform orientation. Therefore, the present research work focuses on functionalizing the MWCNTs with poly(3-hydroxybutyrate) (PHB), a biodegradable polymer which is miscible with chitosan in order to increase the compatibility and dispersion of MWCNTs in chitosan matrix. The result from thermogravimetric analysis (TGA) and transmission electron microscopy (TEM) showed that about 40 wt.% of PHB has been successfully attached to MWCNTs by wrapping on their surface. As to optimize the reinforcing effect from functionalized MWCNT (PHB-MWCNT), it was bulk aligned using simple filtration method. The bulk alignment is found to offer advantages in reducing the amount of MWCNTs required in achieving desired mechanical properties. When applying the PHB-MWCNT/chitosan nanocomposite membranes in dehydration of 1,4-dioxane, the nanocomposite membrane exhibited an increase in selectivity towards water and decreased in



permeate flux when the concentration of 1,4-dioxane in feed solution was increased. However, increasing feed temperature reduced the selectivity of the nanocomposite membranes but improved the permeate flux. When subjected to higher permeate pressure (low vacuum), both the selectivity and permeate flux were decreased due to the reduced driving force. As compared with the chitosan membrane, the incorporation of PHB-MWCNT significantly enhanced the permeability of the membrane but trade off its selectivity. Eventually, the optimum conditions of the nanocomposite membrane in 1,4-dioxane dehydration process were obtained using Response Surface Methodology (RSM). It is suggested that an optimum permeation flux of  $69.48 \text{ g/m}^2\cdot\text{h}$  can be obtained at  $59.7^\circ\text{C}$  feed temperature,  $5.00 \text{ mmHg}$  downstream pressure and  $18.88 \text{ wt.}\%$  of water concentration in feed solution. As for selectivity, the optimal value of  $2292.09$  was predicted at  $30^\circ\text{C}$  feed temperature,  $5.00 \text{ mmHg}$  downstream pressure and  $1.00 \text{ wt.}\%$  of water concentration in feed solution. A balance between the optimum permeation flux and selectivity was estimated to be simultaneously occurred when the pervaporation process was running at  $30^\circ\text{C}$  feed temperature,  $5.00 \text{ mmHg}$  downstream pressure and  $10.92 \text{ wt.}\%$  of water concentration in feed solution. The optimal value of  $40.57 \text{ g/m}^2\cdot\text{h}$  and  $1668.48$  were obtained for permeation flux and selectivity respectively under this operating conditions.

## CHAPTER ONE:

### INTRODUCTION

#### 1.1 Pervaporation

During the past few decades, membrane separation process has become one of the emerging technologies that underwent rapid growth and become an indispensable component in chemical process. Membrane technology constitutes a thin sheet of natural or synthetic material that covers a surface and permeable to a specific component in the solution. The widely used membrane separation processes include microfiltration, ultrafiltration, reverse osmosis, electrodialysis, gas separation and pervaporation. The basic principles of the processes are presented in **Table 1.1**. Most of them are well developed and established. Among them, pervaporation attracts a great deal of interest from researchers and still in rapid development due to low energy required.

Table 1.1: Summary of the membrane separation technologies. (Baker, 2004)

| Process                | Principle  |
|------------------------|--|
| <b>Microfiltration</b> | Separation of organic and polymeric compounds with micropore ranges of 0.1– 10 $\mu$ m                               |
| <b>Ultrafiltration</b> | Separation of water and microsolute from macromolecules and colloids.  |
| <b>Reverse osmosis</b> | Passage of solvents through a dense membrane that is permeable to solvents but not solutes.                          |
| <b>Electrodialysis</b> | Ions are transported through a membrane from one solution to another under the influence of an electrical potential. |
| <b>Gas separation</b>  | Component of mixture of gaseous is removed through a pressure gradient.  |
| <b>Pervaporation</b>   | Component of a mixture diffuses through, evaporates under a low pressure and is removed by a vacuum.                 |

Pervaporation is one of the membrane separation processes for liquid mixtures which involve phase change from liquid to vapor. Generally, it consists of a polymeric membrane that serves as a separating barrier as illustrated in **Figure 1.1**. When a feed liquid mixture contacts with one side of the membrane, one of the components can be preferentially removed from the mixtures in vapor phase as a result of its higher affinity and diffusivity in the membrane. In order to ensure a continuous mass transport, vacuum pump is usually used to maintain low absolute pressure at the downstream side, thereby induce a concentration difference across the membrane. As an alternative, sweeping gas is also used in downstream side to create a driving force and allow the permeate pass through the membrane.

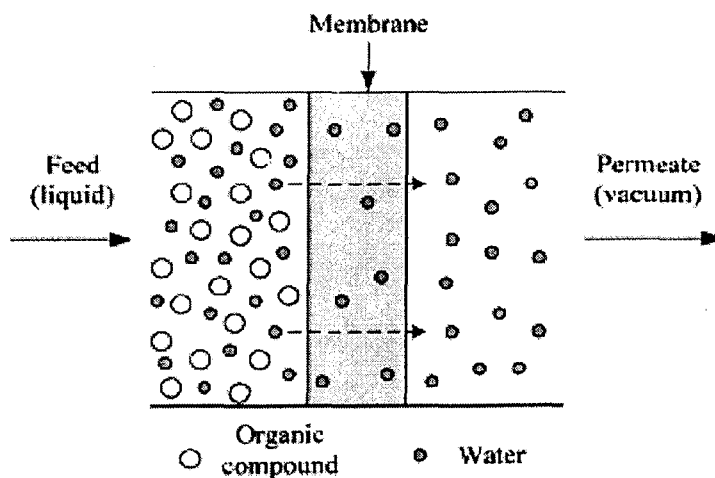


Figure 1.1: Overview of the pervaporation for aqueous organic mixtures.  
(Wee et al., 2008)

Pervaporation is effective in removing the minor component of the liquid mixtures by using the most selective membrane. Instead of conventional distillation, pervaporation is well recognized for its ability to separate azeotropic liquid mixtures because no entrainer is needed. To date, pervaporation has found viable application in the following areas: (i) dehydration of organic solvents (e.g., alcohols, ethers, esters,

acids); (ii) removal of dilute organic compounds from aqueous streams (e.g. removal of volatile organic compounds, recovery of aroma, and biofuels from fermentation broth); (iii) organic-organic mixtures separation (e.g., methyl tert-butyl ether/methanol, dimethyl carbonate/methanol). Among them, dehydration of organic solvents is the best developed.

In pervaporation, selection of membrane materials is essential as the materials critically affect the overall performance. The membrane material is usually selected according to the desired pervaporation process. Pervaporation process can be divided into hydrophilic and organophilic. Hydrophilic pervaporation process involves removal of water from the mixtures. On the other hand, organophilic pervaporation process renders the removal of organic component. Under organophilic pervaporation process, it can be subdivided into hydrophobic and targeted-organophilic. In contrast to hydrophilic pervaporation process, hydrophobic pervaporation process favors the elimination of organic component in organic-water mixtures while target organophilic pervaporation prefer the removal of specific organic component in organic-organic mixtures. The structure of various pervaporation processes is illustrated in **Figure 1.2**.

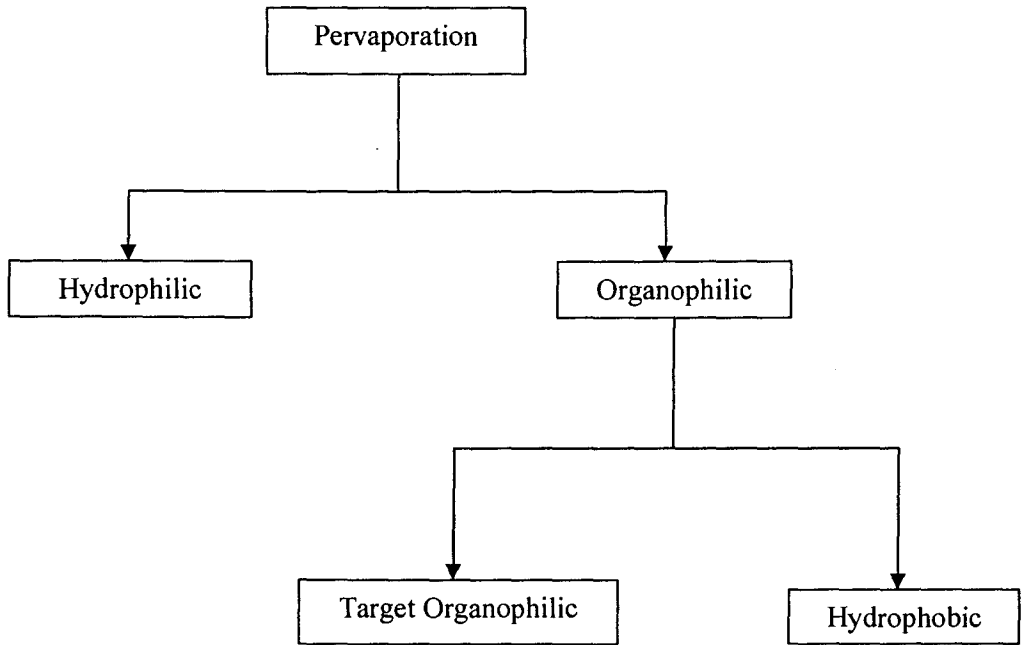


Figure 1.2: Flowchart on different type of pervaporation processes.

Generally, there are three issues must be addressed in developing pervaporation membrane: (i) membrane productivity, (ii) membrane selectivity, and (iii) membrane stability. Membrane productivity is a measurement of the quantity of a component that permeates through a specific surface area in a given unit of time. Membrane selectivity describes the affinity of the membrane toward the specific component and membrane stability defines the ability of a membrane to maintain both the permeability and selectivity under specific system condition for an extended period of time. Usually, most of the pervaporation membranes are made use of synthetic polymer, such as poly(vinyl alcohol) (Xiao et al., 2006) and poly(vinylidene difluoride) (Srinivasan et al., 2007). These polymeric membranes are attractive because they are relatively economical to fabricate (Namboodiri and Vane, 2007).

## 1.2 Biodegradable Polymer

Biodegradable polymers have experienced strong growth over the last three years and are expected to become a strong competitor to conventional thermoplastics in future. The global market for biodegradable polymer is expand at an average annual rate of 13% till 2014 (Interpack, 2010).

According to the American Society for Testing of Materials (ASTM) and the International Standards Organization (ISO), biodegradable polymers can be defined as those undergo a significant change in chemical structure under specific environmental conditions. These changes result in a loss of physical and mechanical properties, as measured by standard methods (Kolybaba et al., 2003). Biodegradable polymers begin their lifecycle as renewable resources, usually in the form of starch or cellulose, and undergo degradation through the action of enzymes and/or chemical decomposition. The degradation temperature which usually falls between 20 to 60°C is depended on the type of active microorganisms (fungi, bacteria, actinomycetes, etc.) with the presence of oxygen, moisture, and mineral nutrient as well as the neutral or slightly acidic (5 to 8) pH conditions (Huang et al., 1990). This degradation process will ultimately leave behind carbon dioxide and water, which are environmentally friendly byproducts. The life cycles of biodegradable polymer is summarized in **Figure 1.3**.

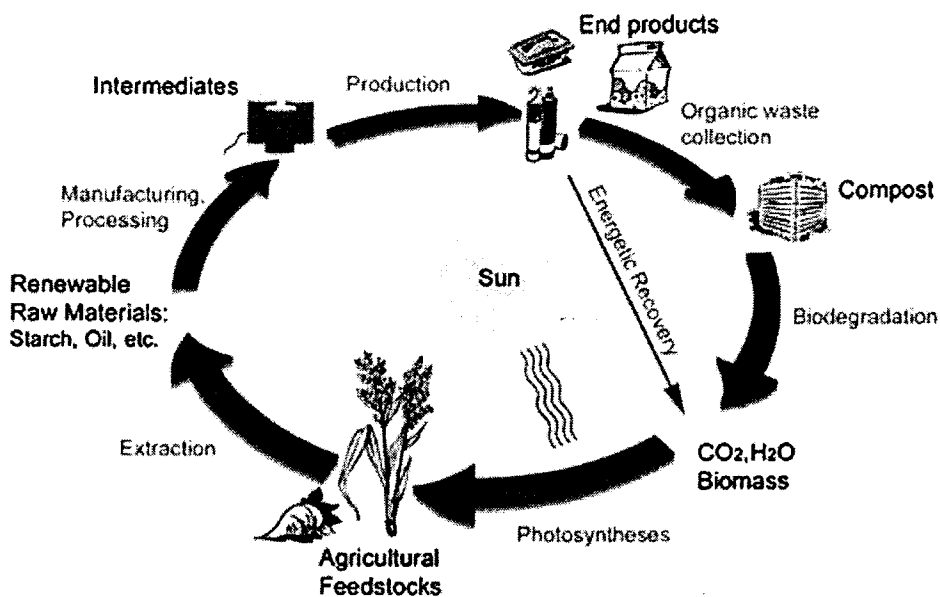


Figure 1.3: Life cycles of biodegradable polymers (Biokam Co, 2008).

Naturally occurring biodegradable polymers are derived from four broad feedstock areas. Animal sources provide collage and gelatin, while marine sources provide chitin which is later deacetylated into chitosan. The remaining two feedstock areas; microbial biopolymer feedstocks and agricultural feedstocks, received the most attention from scientist. Microbial biopolymer feedstocks produce biological polymers through microbial fermentation. The products, including polylactic acid and polyhydroxyalkanoates are naturally degradable, biocompatible and environmentally friendly substitutes for synthetic polymers (Chau and Yu, 1999). On the other hand, polymers from agricultural feedstocks provides starch, a hydrocolloid biopolymer found in a variety of plants including wheat, corn, rice, beans, and potatoes. It is usually utilized in the form of granules, and formed by one branched and one linear polymer. Despite of this, agricultural feedstocks for the biopolymer industry also include fibers that are used as reinforcing fillers. This classification includes cellulose, which is the highly polar, main structural component of flax and hemp fibers (Bismarck et al., 2002).

Since synthetic polymers are resistant to degradation and causing critical issue in waste disposal, European Community suggested a waste management concept based on two complementary strategies: avoiding waste by improving product design and increasing the recycling and re-use of waste with an emphasis in life-cycle assessment (LCA) to generate transparent and complete assessments of environmental impact resulting from all stages of the life cycle of the product or activity in question and to use this to evaluate its environmental attributes (Baillie, 2004). This concept fuels an international drive for the development and application of biodegradable polymer, especially in biomedical field. Biodegradable polymers are preferred candidates for developing therapeutic devices such as temporary prostheses, three-dimensional porous structures as scaffolds for tissue engineering and as controlled/sustained release drug delivery vehicles (Nair and Laurencin, 2007). Each application demands different materials with specific physical, chemical, biological, biomechanical and degradation properties to provide efficient therapy. Apart from that, application of biodegradable polymers in packaging continued to receive more attention. Biodegradable polymer films have shown potential to be employed as garbage bags, disposable cutlery and plate, food packaging, and shipping materials (Kolybaba et al., 2003). The widespread application of biodegradable packaging materials reduces the volume of inert materials that being disposed off in landfills, occupying scarce available space. Furthermore, odor emissions from compost piles are reduced when biodegradable polymers is included in the mix. Thus, research and development to introduce the novel application of biodegradable polymer materials are considered an attractive area as their derivation from renewable sources slowing the depletion of limited fossil fuel stores.



### 1.3 Chitosan

Chitin, poly( $\beta$ -(1 $\rightarrow$ 4)-N-acetyl-D-glucosamine) is a natural polysaccharides that commonly produced in enormous number of living organism in the lower plant and animals kingdom with its structural similar to cellulose, with acetamide groups at the C-2 positions in place of hydroxyl. It is the most abundant organic polymer after cellulose (Honarkar and Barikani, 2009). In industrial processing, chitin is normally extracted from crustaceans by acid treatment to dissolve calcium carbonate followed by alkaline extraction to solubilize proteins. In addition, a decolorization step is often added to remove leftover pigments and obtain a colorless product (Rinaudo, 2006).

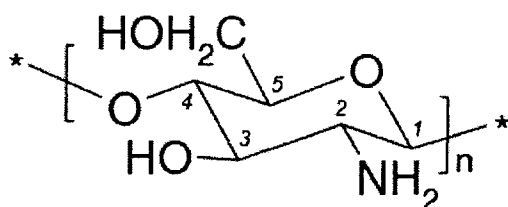


Figure 1.4: Chemical structure of chitosan (Honarkar and Barikani, 2009)

Chitosan is a nontoxic, biodegradable and biocompatible natural polymer that derived through deacetylation of chitin under alkaline condition. It comprises copolymers of glucosamine and N-acetyl glucosamine as shown in Figure 1.4 and the term chitosan embraces a series of polymers which vary in molecular weight (from about 10,000 to 2 million Dalton) (Sanford, 1989). Degree of deacetylation, which represents the proportion of N-acetyl-D-glucosamine units with respect to the total number of units, serves as important factor in determining the physicochemical properties such as crystallinity and solubility. In term of crystallinity, chitosan is counted as semi-crystalline. Maximal crystallinity can be obtained in both chitin (0% deacetylation) and fully deacetylated chitosan (100% deacetylation) while minimal

crystallinity is achieved at intermediate degrees of deacetylation (Şenel and McClure, 2004). The solubility of the chitosan in aqueous acidic media increase with respect to the degree of acetylation due to the protonation of the amine group in C-2 position of the D-glucosamine repeat unit which rendering the conversion of polysaccharide to polyelectrolyte in acidic media (Honarkar and Barikani, 2009). Due to its high molecular weight and linear unbranched structure, the prepared chitosan solution is highly viscous and the viscosity is generally increase with an increase in chitosan concentration at lower temperature and high degree of deacetylation (Şenel and McClure, 2004).

The presence of the amine group enables chitosan to exhibit a variety of physicochemical and biological properties. Its biodegradability and biocompatibility made it a promising substance for application in biomedical field. In addition, it has also found numerous applications in other fields such as waste water treatment, agriculture, cosmetics and food processing. The principal applications of the chitosan are summarized in **Table 1.2**.

Table 1.2: Principal applications of chitosan (Rinaudo, 2006).

| <b>Applications</b>  | <b>Description</b>  |
|----------------------|---|
| Biomedical           | Surgical sutures<br>Dental Implants<br>Artificial skin<br>Rebuilding of bone<br>Time release drugs for animals and humans                               |
| Agriculture          | Defensive mechanism in plants<br>Stimulation of plant growth  |
| Wastewater treatment | Removal of metal ions<br>Ecological polymer (eliminate synthetic polymers)<br>Flocculant to clarify water (drinking water, pools)                       |
| Food processing      | Bind lipids (reduce cholesterol)<br>Preservative<br>Thickener and stabilizer for sauces<br>Protective, fungistatic, and antibacterial coating for fruit |
| Cosmetics            | Maintain skin moisture<br>Treat acne<br>Improve suppleness of hair  |

## 1.4 Problem Statement

Due to good film-forming characteristic and excellent chemical resistant properties, chitosan has been widely used as membrane material for pervaporation separation (Xu et al., 2008, Chapman et al., 2008). However, most of the reports showed that the separation selectivity of chitosan membrane was extremely low owing to its excessive swelling in aqueous solution. Thus chemical or physical modification is necessary to overcome this limitation.

Recently, there has been growing interest in incorporating of carbon nanotubes (CNTs) based fillers into polymeric matrix and applied in pervaporation process. It has been demonstrated that CNTs plays an important role for improving chitosan membrane since CNTs could enhance chemical, mechanical and thermal stability of the chitosan membrane. Significant efforts have been made to incorporate CNTs into chitosan matrix (Liu et al., 2005, Wang et al., 2005). However, producing a high quality CNT/chitosan membrane becomes a daunting task as it requires a homogenous dispersion of CNTs in uniform orientation.

Functionalized CNTs with polymer have been view as an effective way to produce homogeneous CNTs dispersion for better quality polymeric carbon nanocomposite materials. Attachment of specific functional moieties could decrease the van der Waals interaction between CNTs, thereby reduce the formation of agglomerate CNTs and increase the available surface area of the CNTs. In addition, the compatibility between CNTs and the polymer matrix is improved due to the functional moieties enable CNTs to establish covalent coupling of molecule.

Instead of random orientation, a well alignment of CNTs into polymer matrix may optimize the reinforcement effect resulted from good interfacial bonding between the polymer matrix and CNTs. Furthermore, it has been reported that an aligned CNTs within a polymeric film form a nanoporous membrane structure and selectively gate the molecular transport through the ordered nanoporous membrane. This provides the possibility to improve the performance of polymeric membrane in separation process.

Therefore, in this research, incorporation of CNTs into chitosan matrix forming a biodegradable nanocomposite membrane is aim to increase the performance of chitosan membrane in pervaporation process. Method to disperse and align CNTs is developed in order to maximize the quality of the fabricated nanocomposite membrane.

## **1.5 Objectives**

- i. To develop a bulk aligned and dispersed MWCNT/chitosan nanocomposite membrane which is in line with the 3R (Reduce, Reuse and Recycle) concept by a combination of functionalization and simple filtration approach.
- ii. To study the effect of alignment and dispersion of the MWCNTs in the mechanical properties of the nanocomposite membrane.
- iii. To investigate the effectiveness of the nanocomposite membrane in pervaporation process.
- iv. To obtain the optimum condition (temperature, pressure and feed condition) of the nanocomposite membrane in pervaporation process.

## 1.6 Scope of Study

In this study, a pervaporation nanocomposite membrane which comprised of multi-walled carbon nanotube (MWCNTs) and chitosan was produced and applied in the pervaporation process.

The first step in this study was to oxidize and functionalize the MWCNTs with poly (3-hydroxybutyrate) (PHB) as to improve the compatibility of the MWCNTs prior to their incorporation into chitosan matrix. The MWCNTs produced were characterized using thermogravimetric analysis (TGA), fourier transform infrared spectroscopy (FTIR), and etc.

Secondly, process study was carried out by applying the nanocomposite membrane in the pervaporation process and evaluated the effect of the operating parameter (feed temperature, feed concentration and downstream pressure) on the pervaporation performance (permeation flux and selectivity).

Lastly, the optimum conditions of the pervaporation process were conducted using response surface methodology (RSM) coupled with central composite design (CCD) in Design-Expert Version 6.0.6 software.

## 1.7 Organization of the Thesis

This thesis will be divided into five chapters. In each chapter, it will contain relevant parts that corresponds its chapter's title and each will also contain the information of the research.

Chapter one will explain on the general overview of the pervaporation process. Simple introduction on biodegradable polymers and chitosan were included as well as to supply some information of the related materials. After that, problem statement was highlighted to address the issue regarding the limitations of chitosan membrane in pervaporation process and suggestion to overcome them. It was then follow by the objective clearly stated out the purpose of this research project. Finally, the organization of the thesis highlights the content for each chapter.

Chapter two presents the overall literature review of various research works reported in the literature in this research area. Initially, fundamental information of CNTs including brief introduction on CNTs structure, recent technology to produce CNTs and their unique properties were reported. Subsequently, various research works related to the application of CNTs as reinforcement, recent technique in dispersing and aligning CNTs were reviewed. Apart from that, fundamental of the pervaporation process and studies on chitosan as pervaporation membrane were also included. At the end of this chapter, the use of RSM in the optimization of the pervaporation was discussed.

In chapter three, experimental materials and methodology were discussed. The details information on how to conduct the experimental work was reported and

overview of the experimental work done was expressed in a flowchart. The method and equipment used for characterization were described. The required equation for data analysis was also provided.

Chapter four plays a major role in this thesis. It reveals the outcome of the research. The detail on the result and the discussion was presented in this chapter. This chapter is divided into two sections according to the stage of the project. In the first section, there will be a discussion on result and characterization of the resulted CNTs. In second section, it will mainly focus on the biodegradable CNTs based nanocomposite membrane. Evaluation of the membrane's properties and its performance in term of pervaporation process as well as the optimization study on the pervaporation process were reported.

At last, the outcomes obtained are presented in chapter five. Based on the result and discussion, the conclusions of the research project were made and recommendations for the future studies related to this research project were provided.



## CHAPTER TWO: LITERATURE REVIEW

### 2.1 Brief Introduction on Carbon Nanotubes

Since the discovery of carbon nanotubes (CNTs), they have attracted the attention to revolutionize the future nanotechnologies area. CNTs as reported by Iijima (1991) and Bethune (1993) group, are seamless macromolecules with a radius as small as a few nanometers, and up to several micrometers in length. The walls of these tubes consist of the hexagonal lattice of carbon atom and their ends are usually capped by fullerene-like structures. The unique structure of CNTs can be divided mainly into multi-walled carbon nanotubes (MWCNTs) and single-walled carbon nanotubes (SWCNTs). MWCNTs was the first nanotubes observed which consist of two or more concentric cylindrical shells of graphene sheets coaxially arranged around a central hollow area with a spacing between the layer which is close to that of the interlayer separation as in graphene. In contrast, SWCNTs are made of single cylinder graphite sheet held together by van der Waal's bond (Daniel et al., 2007, Balasubramanian and Burghard, 2005). Structure of SWCNTs can be distinctly unique as there are many ways to roll a graphene sheet into a SWCNTs and commonly can be categorized into 3 different conformations by a pair of  $(n,m)$  integers corresponding to the specific atoms on a planar graphene sheet and an angle of helicity,  $\theta$ . Armchair conformation, denotes by  $(n,n)$  tubes, occurring when  $\theta = 30^\circ$ , its plane symmetry parallel to the nanotube axis. The  $(n,0)$  nanotubes with  $\theta = 0^\circ$ , give zigzag conformation whereby its plane symmetry is perpendicular to the nanotube axis. Both conformations can be referred as "achiral" nanotubes. All the other vectors  $(n,m)$  correspond to  $0 < \theta < 30^\circ$ , where  $n \neq m \neq 0$  are correspond to

chiral tubes since they are unable to be superimposed on their own image in mirror like those achiral tubules. Schematic on different conformation of CNTs are shown in **Figure 2.1**.

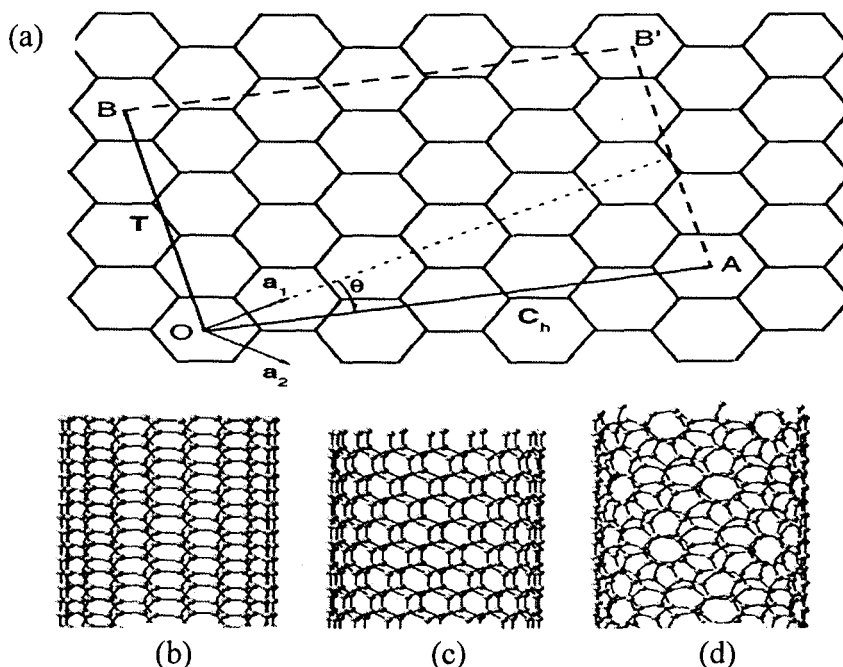


Figure 2.1: (a) Schematic diagram showing the possible wrapping of the 2D graphene sheet into tubular forms, (b) an armchair-type nanotube, (c) a zigzag type nanotube, and (d) a chiral-type nanotube. (Popov, 2004)

Production of CNTs addresses a challenge in adapting to the economically feasibility and specifically control the configuration (chirality), purity and structure quality. Current synthesis techniques including electric arc discharge (Journet et al., 1997), laser ablation (Guo et al., 1995) and chemical vapor decomposition (CVD) (Dai et al., 1996) are commercially used to produce large quantity of CNTs. The overview of the synthesis procedures are listed in **Table 2.1**.

Table 2.1: Overview of the important synthesis procedures for carbon nanotubes. (Balasubramanian and Burghard, 2005)

| Synthesis method                          | Principle   | Maximum production rate |
|---|---|-------------------------|
| <b>Electric arc-discharge</b>             | Carbon atoms are generated through an electric arc discharge at $T > 3000^{\circ}\text{C}$ between two graphite rods. Nanotubes are formed in the presence of suitable catalyst metal particles (Fe, Co, or Ni).  | 120 g/day               |
| <b>Laser ablation</b>                     | Generation of atomic carbon at $T > 3000^{\circ}\text{C}$ through laser irradiation of graphite, which contains appropriate catalyst particles (Fe, Co, or Ni), is followed by formation of nanotubes.  | 50 g/day                |
| <b>Chemical vapor decomposition (CVD)</b> | Decomposition of a gaseous hydrocarbon source (e.g., an alkane or CO) is catalyzed by metal nanoparticles (Co or Fe). Particles are prepared by pyrolysis of suitable precursors (e.g., $[\text{Fe}(\text{CO})_5]$ ) at $1000\text{-}1100^{\circ}\text{C}$ under high pressure. | 50 g/day.               |

## 2.2 Properties of Carbon Nanotubes

The unique mechanical, electrical and chemical properties of CNTs are strongly depend on their structural conformation and hybridization state (Ajayan, 1999). The ground state orbital configuration of carbon's electrons is  $1s^2, 2s^2, 2p^2$ . The narrow gap between the 2s and 2p electron shells facilitates the promotion of s orbital electron to higher energy p orbital that is empty in the ground state, which render the carbon atom to hybridize into  $sp$ ,  $sp^2$ , or  $sp^3$  (Hu et al., 2007).

CNTs possess high stiffness and axial strength which make them particularly stable against deformation attributed to the strong chemical bond between carbons atom. Apart from that, CNTs are found to behave flexible as their hexagonal network that capable to distort for relaxing stress. Tensile loading test performed by Yu et al.

(2000) on CNTs reported that the tensile strength value for SWCNTs ranging from 13 to 52 GPa and MWCNTs were in the range from 11 to 63 GPa. Measurement of Young's modulus value was conducted through both theoretical prediction and experimental measurement. The experimental measurements performed by using vibration spectroscopy, atomic force microscopy (AFM), and transmission electron microscopy (TEM) obtained an average value of 1.8 TPa (Jacobsen et al., 1995). While the theoretical prediction, which was calculated through simulation studies was in the range of 1-5 TPa. It is realized that the CNTs Young's modulus is much higher compared with typical carbon fibers (Cornwell and Wille, 1997).

CNTs demonstrated distinctly different electronic properties depending on their conformations. Early calculation predicted that their metallic and semiconducting properties are greatly defined by their chirality and diameter. Theoretical and experimental work showed that armchair conformation denoted by (n,n) tubes are metallic (zero band gap) while the zigzag and chiral conformation (n,m) give small gap or large gap semiconducting properties (Dresselhaus et al., 2001). It has been experimentally confirmed that CNTs behave like a quantum wire intrinsically because of the electron confinement effect quantizing the conduction band into discrete energy levels. Electrons are transported via resonant tunneling through these discrete electron states and delocalized over certain length of the CNTs. This spatial extension of charge not only enhances conductivity and current capacity, but also reduces the influence of defect in CNTs sidewalls (Mauter and Elimelech, 2008).

Similar with graphite and diamond, CNTs exhibit an extraordinary heat capacity and thermal conductivity properties depending on temperature. The thermal conductivity in CNTs is primarily determined by phonons. At low temperature, the effects of phonon quantization cause an unusual behavior in CNTs thermal conductivity. The thermal conductivity of CNTs reflect the on-tube phonon structure and the measurement of the thermal conductivity of bulk samples show graphite-like behavior for MWCNTs but quite different behavior for SWCNTs. Theoretical prediction and experimental measurements showed that the thermal conductivity for CNTs at room temperature could be vary between 1800 and 6000 W/m·K and the thermal properties of CNTs is strongly dependence on the sample quality and alignment (Meyyappan, 2004).

In short, both theory and experiment show extraordinary structures and properties of CNTs. The small dimensions, strength and the remarkable chemical and physical properties of these structures enable the application for CNTs as reinforcing agent in fabricating high strength composite with multi-functional properties.

### **2.3 Carbon Nanotubes as Reinforcing Agent in Polymer Nanocomposite**

Since the first CNT/polymer nanocomposite developed by Ajayan et al. (1994), there has been a growing interest in applying CNTs as reinforcing agent to form a nanocomposite with desired characteristic. The number of published journal articles related to the CNT/polymer nanocomposite has gradually increased within this decade as shown in **Figure 2.2**. CNTs are said to be stiffer than steel, lighter than aluminum and more conductive than copper. Therefore the unique mechanical, electrical and thermal properties made them an excellent candidate to substitute the

conventional reinforcing agent in the fabrication of multifunctional polymer nanocomposite.

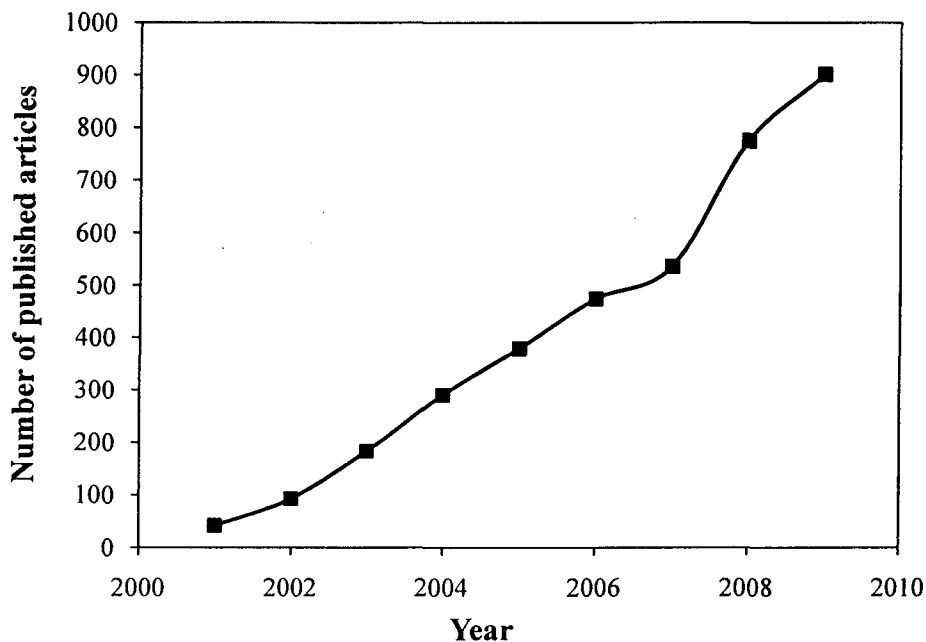


Figure 2.2: Number of published journal articles relate to CNT/polymer nanocomposite as a function of year (Data obtained through the ISI web of knowledge search).

Light nanocomposites are expected upon the incorporation of CNTs into polymer matrix because of their low mass density, large aspect ratio, high strength and flexibility. Since CNTs are capable to sustain huge energy loading, they will assist to bear the load from the polymer when the nanocomposite undergoes mechanical stress, hence improved the tensile strength. Though tensile strength and modulus of the nanocomposite are increased with respect to the amount of CNTs, however too high CNTs loading will cause insufficient impregnation of the polymer within the CNTs network, thereby reduce the reinforcing effect (Tai et al., 2008). Generally, desired mechanical properties in nanocomposite can be easily achieved at relative low CNTs concentration by taking advantages of their large surface area. Geng et al. (2002) have obtained a 145% of tensile-modulus improvement with the

addition of 1 wt.% CNTs in a poly(ethylene oxide) (PEO). Nevertheless, fatigue damage resistance possessed by CNTs allow significant enhancement in fracture toughness of the nanocomposites. Grimmer et al. (2008) observed that incorporating CNTs into epoxy matrix tends to inhibit the damage propagation since CNTs provide a large density of fatigue crack initiation site.

In term of electrical properties, addition of CNTs in composite containing conducting polymer could enhance the conductivity and electron transport ability. Such improvements envision the wide application for the conductive composite, including electrostatic painting and electromagnetic interference shielding (Moniruzzaman and Winey, 2006). The onset of electrical conductivity in a CNT/polymer nanocomposite occurs when CNTs content exceed a critical value, known as percolation threshold. The percolation threshold is characterized by a sharp jump in the conductivity by many orders of magnitude attributed to the conductive pathway formed by conductive fillers. It is typically determined by plotting the electrical conductivity as a function of CNTs mass fraction which is fitting with a power law function. The percolation threshold for the electrical conductivity in CNT/polymer is highly influenced by several characteristics of CNTs: type of CNTs (SWCNTs or MWCNTs), aspect ratio, state of dispersibility, presence of functional group, specific surface area and the concentration of CNTs (Moniruzzaman and Winey, 2006). Attributed to the high aspect ratio, CNTs manage to impart electrical conductivity in epoxy matrix at an average loading of 0.005 wt.% (Sandler et al., 2003). Although it is widely accepted that attachment of the functional group disrupts the extended  $\pi$ -conjugation of CNTs, thereby reduce the electrical conductivity, several researchers have reported an opposite effects when

incorporated functionalized CNTs into polymer matrix. Valentini et al. (2004) pointed out that the amine-functionalized CNTs in epoxy matrix promote migration of intrinsic charges, which enhanced the electrical conductivity. Tamburri et al. (2005) demonstrated an improvement of current in poly(1,8-diaminophthalene) by a factor of 90 and 140 after the incorporation of SWCNTs with -OH and -COOH functional group, whereas the pristine CNTs showed an enhancement of only 20. It seems that the existence of functional group greatly enhanced the conductivity of CNTs due to good dispersion, hence the disadvantage resulted from the functional group as stated earlier is outweighed.

On the other hand, many researchers have found an improved thermal stability in CNT/polymer nanocomposite. The low thermal conductivity exhibited by polymer made them hardly sustain at high temperature condition. Thus, addition of CNTs into polymer matrix forms a physical barrier effect to hinder the flux of thermal degradation. Investigation in CNT/poly(L-lactide) nanocomposite showed a higher thermal degradation peak temperature and onset temperature of degradation along with a higher amount of residue at the completion of degradation than neat PLLA (Kim et al., 2009). Srivastava et al. (2009) reported that the degradation temperature of polyaniline shifted to higher temperature up to 600°C upon the incorporation of CNTs. Similar effects also observed in CNT/poly(butylenes terephthalate) nanocomposite as the incorporation of CNTs increase the activation energy for thermal decomposition, create a physical barrier effects against thermal decomposition and lead to the enhancement of thermal stability. Another possible mechanism of the improved thermal stability in CNT/polymer nanocomposite is attributed to the unusual high thermal conductivity of CNTs which facilitates heat



dissipation within the nanocomposites (Kim, 2009). The thermal stability of the nanocomposite is found to improve with better dispersion, high loading, and high aspect ratio of CNTs.

#### **2.4 Fabrication of Carbon Nanotube/Polymer Nanocomposite**

Fabrications of CNT/polymer nanocomposite have overwhelmingly focused in improving their quality. Techniques including physical blending and in-situ polymerization were widely applied to improve the properties of these nanocomposites.

Physical blending is the most common technique to fabricate polymer nanocomposites. This technique had been applied to prepare polymer composite with micron-sized filler in early day and is still amenable and effective when nano-sized filler are considered to replace the micron-sized filler. In general, there are two types of physical blending: solution blending and melt blending. Solution blending involves two major steps: dispersed CNTs in polymer solution (at room temperature or elevated temperature), and recover the nanocomposites by precipitating or casting into a film. The use of high power sonication appears as the simplest and convenient way to achieve homogenous dispersion of CNTs in polymer. For example, Qian et al. (2000) able to dispersed CNTs uniformly in polystyrene matrix by made use of high energy sonication. When comes to nanocomposites recovery, CNTs tend to agglomerate back into bundle when the solvent evaporation time is long, lead to inhomogeneous distribution of CNTs in polymer matrix. In order to overcome this limitation, the evaporation time can be reduced by dropping CNT/polymer solution on a hot substrate such as hotplate. As an alternative option, Du et al. (2003)